Integrated magnetooptic cross strip isolator

*M. Lohmeyer**

MESA$^+$ Research Institute, University of Twente, Enschede, The Netherlands

L. Wilkens, O. Zhuromskyy, H. Dötsch, P. Hertel

Department of Physics, University of Osnabrück, Osnabrück, Germany

Abstract: A bimodal planar waveguide segment of specific length and thickness between two thinner single mode sections can serve as an interferometer. Depending on the phase gain of the two modes in the thick region, these fields can interfere destructively or constructively at the transition from the bimodal to the single mode section. We employ this geometry to realize a simple magnetooptic isolator configuration, using a wide strip that is etched into a double layer in-plane magnetized magnetooptic film. The magnetization is oriented parallel to the strip; the light traverses the strip perpendicularly. Then the magnetooptic effect causes the phase velocities of TM polarized waves to be different for opposite directions of light propagation, resulting in a nonreciprocal power transfer across the strip. For a properly selected geometry one can expect isolator performance. If the strip width varies slightly, then adjusting the beam incoupling position means to change the distance which the light travels in the two mode segment. This offers a convenient tuning possibility, which may be a means to overcome the strict fabrication tolerances that apply usually to interferometric integrated isolator concepts.

Keywords: integrated optics, magnetooptic waveguides, Faraday effect, optical isolators
PACS codes: 42.82.–m 42.82.Et 85.70.Sq 78.20.Ls

1 Introduction

Despite an ongoing demand in the field of optical telecommunication, experimental realizations of integrated optical isolators are still rare. Being intended to pass the optical power in one direction of light propagation but to block the power transmission for the opposite direction, optical isolators find their most prominent application in protecting a laser from the light that is backscattered by the attached optical circuit.

Analogously to their micro- or bulk-optic counterparts, earliest concepts for integrated optical devices rely on the Faraday-effect, the nonreciprocal polarization conversion caused by a magnetooptic material with the magnetization oriented parallel to the direction of light propagation [1, 2, 3]. If the magnetization is adjusted perpendicularly to that direction, the magnetooptic anisotropy shows up in different phase velocities of counterpropagating waves, the nonreciprocal phase shift. First for TM polarized waves [4, 5, 6], later for TE fields [7, 8, 9], and recently aiming at a polarization independent performance [10, 11], these phase shifts constitute the basis for a number of isolator proposals relying on nonreciprocal interferometry. A common difficulty with all these designs are very strict fabrication tolerances. While the nonreciprocal polarization converters require a phase matching condition to be precisely observed [3], the larger device length of the interferometric concepts leads to difficulties in adjusting the intrinsic phase [12, 5]. Both conditions show up in very narrow limits for the waveguide geometries. Consequently, an integrated isolator device has to include a tuning facility, at least for the magnetooptic materials that are currently available.

This paper addresses the task using a simple planar geometry that has been proposed with the background of a polarizer design in Ref. [13]. Avoiding the necessity to include polarizers, power splitters, or laterally precisely dimensioned (bend) waveguides, the concept should be superiour to many of the previous proposals in terms of manufacturing effort. Figure 1 sketches the relevant structure. It consists of a wide strip, deeply etched into a magnetooptic film. A beam of light — unguided in the lateral direction, guided in the direction normal to the film — is made to cross the strip perpendicularly. Provided that the geometric dimensions are properly selected, the device has the transmission characteristics of an interferometer. This is illustrated in Section 2, where we consider the light propagation in terms of a simple overlap model. Section 3 focuses on the isolator application.

* *Faculty of Mathematical Sciences, University of Twente* *P.O. Box 217, 7500 AE Enschede, The Netherlands*
Phone: +31/53/489-3448 *Fax: +31/53/489-4888* *E-mail: m.lohmeyer@math.utwente.nl*

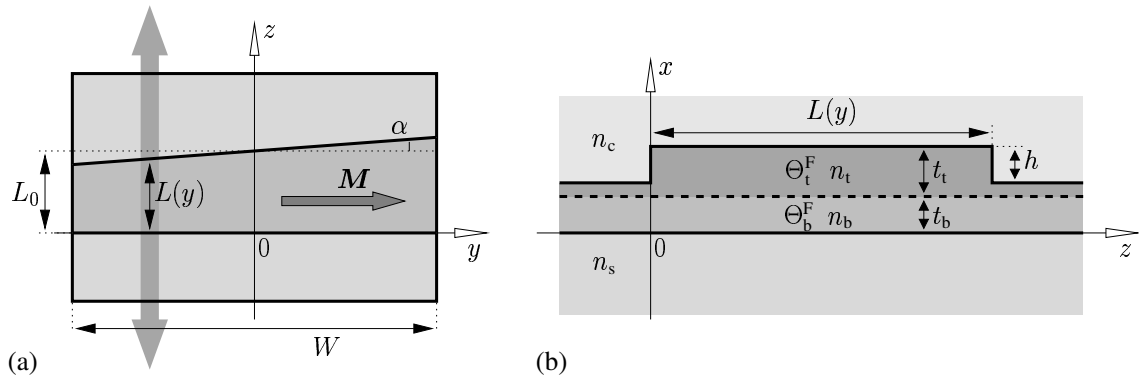

Figure 1: Top view (a) and x-z-cut (b) of the magnetooptic cross strip interferometer. x and y denote the transverse coordinate axes, with the x-direction normal to the film plane. Light propagates along the z-direction. The double layer waveguide with film thicknesses t_b and t_t consists of two magnetooptic layers with opposite Faraday rotations Θ_b^F and Θ_t^F, with the magnetization $\boldsymbol{M}$ oriented along the y-axis. n_s, n_b, n_t, and n_c are the refractive indices of the substrate, the guiding film, and the cover, respectively. The wide strip of width W and height h is perpendicular to the direction of light propagation, with the front and back edges adjusted at a small angle α. A beam injected at position y passes through a double layer section of length $L(y)$.

Since this is essentially a planar concept, the freedom in the lateral direction can be exploited for tuning the device. That is the subject of Section 4. Finally, Section 5 shows the results of a more rigorous simulation that includes the radiated and reflected parts of the electromagnetic fields.

2 Cross strip interferometer

For a fixed vacuum wavelength λ, all parameters introduced in the caption of Figure 1 shall be selected such that the etched input and output regions $z < 0$, $z > L(y)$ of the device constitute vertically single mode waveguides, while the strip region in between supports two guided modes. For small strip angles α and modestly laterally focused input light both the optical fields and the permittivity are approximately constant in the y-direction. Hence for the present the simulation of the light propagation can be restricted to one transverse dimension. The effects of the trapezoidal strip shape and of finite beam widths are considered in Section 4.

Only TM polarized fields are of interest in the present context. Disregarding for the moment the magnetooptic properties of the material, for a simple overlap model only a few ingredients are required. ψ denotes the guided mode profile of the input and output segments. ϕ_0 and ϕ_1 are the fundamental and first order mode of the coupling section; β_0 and β_1 are the corresponding propagation constants. The modes are meant to be normalized with respect to a proper scalar product $(\ .\ ,\ .\ )$. See Ref. [13] for a specification of the abstract notation. Assuming that a normalized input field passes a thick segment of length L, by equating transverse components at the two waveguide junctions, projecting on the involved fields, and using the orthogonality properties for guided modes, one arrives at the following expression for the relative power transmission:

$$P(L) = w_0^2 + w_1^2 + 2w_0 w_1 \cos(\beta_0 - \beta_1)L\,. \tag{1}$$

The factors w_0, w_1 are the squared mode overlaps $w_j = (\psi, \phi_j)^2$, which are real for suitably chosen basic mode profiles.

The transmitted power varies strictly harmonically with respect to the length L of the strip segment, with a half beat length or coupling length $L_c = \pi/(\beta_0 - \beta_1)$. Obviously the maximum respectively minimum throughput is given by the sum $(w_0 + w_1)^2$ or the difference $(w_0 - w_1)^2$ of the overlaps. Hence one can expect interferometric behaviour of the device — i.e. alternatively almost complete or no power transmission — if the geometric parameters can be adjusted such that the overlaps are equal, while at the same time their sum is as large as possible. For the isolator application, the condition $w_0 = w_1$, implying the complete suppression of the power transmission, is essential. We have found, that proper adjustment is indeed possible for a specific range of total thicknesses $t_b + t_t$ by selecting a suitable etching depth h. Figure 2 shows examples for the involved mode profiles and their superpositions.

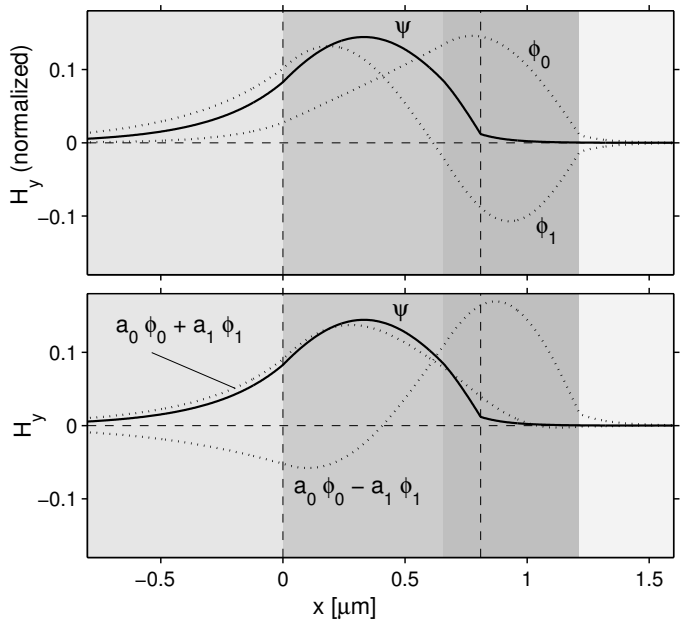

Figure 2: Basic magnetic field component H_y of the TM modes for the structure defined by the parameters of Table 1. Top: The mode ψ of the input/output waveguide, and the profiles corresponding to the two guided modes ϕ_0, ϕ_1 of the coupling segment. Bottom: With suitable amplitudes $a_j = \sqrt{w_j} = 0.703$, the modes of the thicker waveguide form a field that matches the output mode well (+), or that is orthogonal to the output profile (−). The shading indicates the permittivity of the coupling segment, while the vertical lines mark the boundaries of the input/output core.

For a properly adjusted geometry a symmetric superposition of ϕ_0 and ϕ_1 can be reasonably close to the input and output mode ψ. Therefore little power is lost, if this field excites the strip region at $z = 0$, or if the symmetric superposition arrives at the output junction in $z = L$. At the same time, the antisymmetric superposition of ϕ_0 and ϕ_1, with absolute values of the amplitudes as before, but with an additional phase difference of π, is orthogonal to ψ. Hence the output mode does not receive any power, if this superposition excites the lower region at $z = L$. In that case the power is partly reflected, but mostly radiated away, a smaller part into the cover, a larger fraction into the higher index substrate.

Consequently, a simulation of the interferometer should take these effects into account. However, we observed that the overlap model describes the situation well enough for the device design. A refined mode expansion simulation in Section 5 and similar calculations of single junctions in Ref. [13] confirm and illustrate the expected behaviour.

3 Cross strip isolator

Besides the guiding refractive index, there is a second contribution to the permittivity, which accounts for the magnetooptic properties of the film material. With the static magnetization oriented in the film plane perpendicular to the direction of light propagation, the primary effects of this magnetooptic anisotropy are nonreciprocal phase shifts for TM polarized fields, i.e. the propagation constants for modes propagating in positive and negative z-direction differ [14, 15]. If relevant, indices $d = \mathrm{f}, \mathrm{b}$ for forward and backward propagation specify the direction. While in principle this applies to propagation constants as well as to mode profiles, by computing the exact analytical mode solutions for the magnetooptic waveguide [16] one observes that the small change of the mode profiles with the direction of propagation is clearly negligible. Thus the magnetooptic effect can be modelled adequately in the framework of perturbation theory [14, 17], using the mode profiles of the basic isotropic structure. As before, all quantities are assumed to be constant along the y-direction. Section 4 shows that the angled strip geometry, together with limited beam width, allows to meet the critical condition for isolator performance, which will be established in the next paragraph.

Along with the propagation constants β_0^d, β_1^d, the coupling lengths L_c^d differ for forward and backward transmission, and one can expect a nonreciprocal behaviour of the power throughput as well: $P^\mathrm{f} \neq P^\mathrm{b}$. The isolator device has to be assessed in terms of the isolation ratio $\mathrm{IS} = 10 \log_{10} P^\mathrm{f}/P^\mathrm{b}$ and loss $\mathrm{LO} = -10 \log_{10} P^\mathrm{f}$. Hence for optimal performance, the length L of the strip segment should match at the same time an even multiple of the forward coupling length and an odd multiple of the backward coupling length: $L = 2mL_\mathrm{c}^\mathrm{f} = (2m \pm 1)L_\mathrm{c}^\mathrm{b}$.

This allows to compute a characteristic length

$$L_{\rm is} = \frac{L_{\rm c}^{\rm f}\, L_{\rm c}^{\rm b}}{|L_{\rm c}^{\rm f} - L_{\rm c}^{\rm b}|} = \frac{\pi}{|(\beta_0^{\rm f} - \beta_0^{\rm b}) - (\beta_1^{\rm f} - \beta_1^{\rm b})|} \tag{2}$$

for the isolating interferometer. A short device needs the difference between the forward and backward coupling lengths to be large. According to the second equality, this requires a pronounced difference in the nonreciprocal phase shifts $\beta_j^{\rm f} - \beta_j^{\rm b}$ of the two modes. Therefore, our design rests on a double layer structure with opposite signs of the Faraday rotation in the two magnetooptic films. If the central boundary at $x = t_{\rm b}$ is placed close to the field maximum of ϕ_0 respectively to the zero of ϕ_1, the fundamental mode is subject to a large nonreciprocal phase shift, while the first order mode remains almost unaffected by the magnetooptic perturbation. See e.g. Ref. [17, 15] for details on the optimization of the effect.

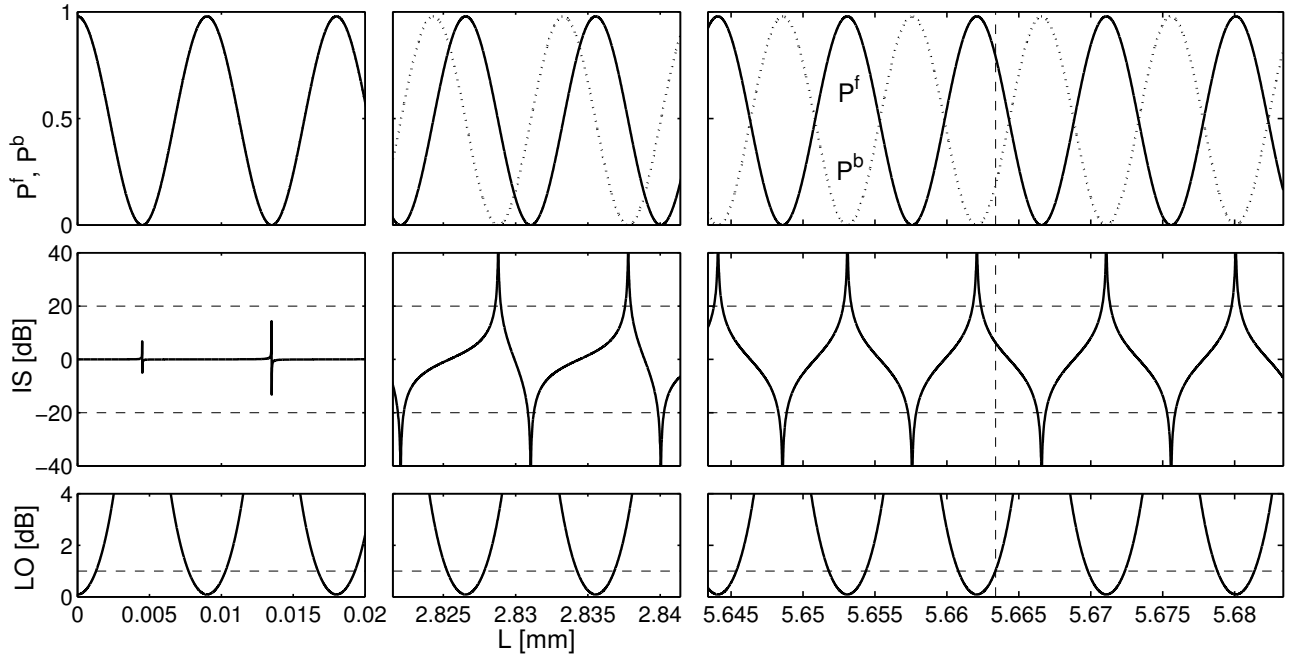

Figure 3: Forward and backward power transmissions P^f, P^b, isolation IS and loss LO versus the length L of the double layer segment. Parameters are as stated in Table 1. The vertical line is placed at the length $L_{is} = 5.663$ mm.

Figure 3 shows the dependence of the characterizing quantities on the length L of the coupling section for a very narrow strip, for L around $L_{\rm is}/2$, and for L around $L_{\rm is}$. Usually, best conditions do *not* occur, if L matches $L_{\rm is}$ exactly, since the condition of $L_{\rm is}/L_{\rm c}^{\rm f}$ (or $L_{\rm is}/L_{\rm c}^{\rm b}$, resp.) being an integer number does not enter the definition (2). $L_{\rm is}$ indicates a length, where the harmonic curves related to $P^{\rm f}(L)$ and $P^{\rm b}(L)$ are out of phase exactly by π. But since there is only a small difference between $L_{\rm c}^{\rm f}$ and $L_{\rm c}^{\rm b}$, i.e. the phase difference changes only very slowly with L, close to $L_{\rm is}$ one can find lengths with simultaneously almost zero $P^{\rm b}$ and high $P^{\rm f}$, thus with — in the framework of the present model — ideal isolator performance. $L_{\rm is}$ is therefore a reasonable choice for the basic strip width L_0.

4 Tuning and tolerances

As exemplified by the structure of Table 1, an interferometer of a length of about 5.6 mm will have to distinguish between 1258 forward half-beats and 1259 coupling lengths in the backward direction. This necessarily requires a postfabrication tuning possibility, which for the present proposal can be found in the lateral beam incoupling position y. We refer now to Figure 1(a). Assume that the lateral extension of the device W, the basic strip width L_0, and the strip angle α are selected such that the interval $[L_0 - (W/2)\tan\alpha, L_0 + (W/2)\tan\alpha]$ includes a few coupling lengths around $L_0 = L_{\rm is}$. Then the light that is coupled in at position y passes a cross strip interferometer of length $L(y) = L_0 + y\,\tan\alpha$. For a few small strip angles, Figure 4 depicts the y-dependence

of the relevant quantities. By shifting the incoupling position (on a macroscopic scale), one can always prepare a configuration where the isolator performance is in a local maximum.

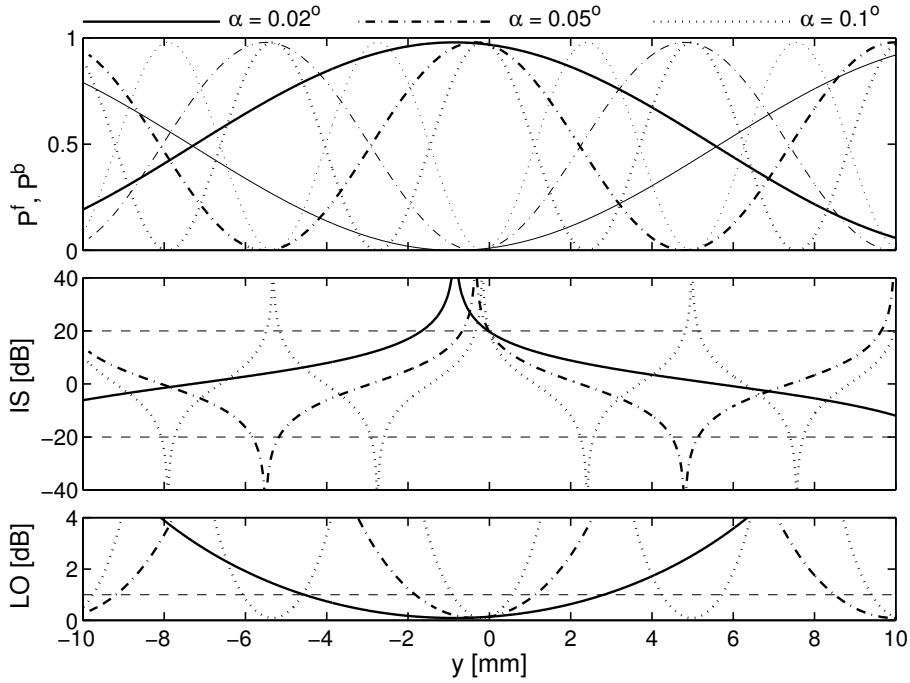

Figure 4: Forward and backward power transmissions P^{f} (bold lines), P^{b}, isolation IS and loss LO for different strip edge angles α versus the beam incoupling position y. The locally relevant length L of the double layer segment is $L(y) = L_0 + y\tan\alpha$. See Table 1 for parameters.

Note that the curves of Figure 4 are to be expected if one assumes a beam of a small width, which is negligible on the lateral scale. With necessarily finite beam width the values have to be averaged over a specific y-interval. The figure proves, that one can still expect reasonable isolator performance (provided that the strip edge angle α has been properly selected) even for beam widths e.g. about 1 mm, which are very large on the integrated optics scale.

Hence, to estimate the tolerances of the cross strip isolator experiment, we may concentrate on the variations of the local isolation maxima or the corresponding loss, respectively, disregarding the short range dependence of these quantities on L. For this purpose, the expressions for the isolation ratio and loss are rewritten in the following form:

$$\mathrm{IS}(L) = 10\log_{10}\frac{w_0^2 + w_1^2 + 2w_0w_1\cos\left(\pi\,L/L_{\mathrm{c}}^{\mathrm{b}} + \pi\,L/L_{\mathrm{is}}\right)}{w_0^2 + w_1^2 + 2w_0w_1\cos\left(\pi\,L/L_{\mathrm{c}}^{\mathrm{b}}\right)}\,, \tag{3}$$

$$\mathrm{LO}(L) = -10\log_{10}\left(w_0^2 + w_1^2 + 2w_0w_1\cos\left(\pi\,L/L_{\mathrm{c}}^{\mathrm{b}} + \pi\,L/L_{\mathrm{is}}\right)\right)\,.$$

There is a rapid oscillation of $\mathrm{IS}(L)$ and $\mathrm{LO}(L)$ with a characteristic length $L_{\mathrm{c}}^{\mathrm{b}} \approx L_{\mathrm{c}}^{\mathrm{f}}$, modulated by a slower oscillation with characteristic length L_{is}. If $w_0 \approx w_1$, the isolation maxima are located at the lengths $L = (2m+1)L_{\mathrm{c}}^{\mathrm{b}}$, natural m, where the denominator of IS is minimal. At these points, isolation and loss are approximately

$$\widetilde{\mathrm{IS}}(L) = 10\log_{10}\frac{w_0^2 + w_1^2 - 2w_0w_1\cos\left(\pi\,L/L_{\mathrm{is}}\right)}{\left(w_0 - w_1\right)^2}\,, \tag{4}$$

$$\widetilde{\mathrm{LO}}(L) = -10\log_{10}\left(w_0^2 + w_1^2 - 2w_0w_1\cos\left(\pi\,L/L_{\mathrm{is}}\right)\right)\,.$$

$\widetilde{\mathrm{IS}}(L)$ and $\widetilde{\mathrm{LO}}(L)$ vary but slowly on the tuning range $W\tan\alpha$. Hence adjusting the beam position y always permits to realize a configuration where approximately $\mathrm{IS}(L(y)) = \widetilde{\mathrm{IS}}(L_0)$ and $\mathrm{LO}(L(y)) = \widetilde{\mathrm{LO}}(L_0)$. With the basic strip width chosen as $L_0 = L_{\mathrm{is}}$, these quantities evaluate to $\widetilde{\mathrm{IS}}(L_0) = 10\log_{10}((w_0+w_1)^2/(w_0-w_1)^2)$ and $\widetilde{\mathrm{LO}}(L_0) = -10\log_{10}(w_0+w_1)^2$.

	q	Δq
t_b	$0.656\,\mu$m	$\geq 0.2\,\mu$m
t_t	$0.559\,\mu$m	$0.16\,\mu$m
h	$0.405\,\mu$m	30 nm
L_0	5.663 mm	1.6 mm
λ	$1.3\,\mu$m	≥ 90 nm

	q	Δq
n_s	1.950	0.1
n_b	2.157	0.02
n_t	2.275	0.02
n_c	1.0	≥ 0.4
$\Theta_\mathrm{b}^\mathrm{F}$	$150°/\,\mathrm{cm}$	$202°/\,\mathrm{cm}$
$\Theta_\mathrm{t}^\mathrm{F}$	$-1000°/\,\mathrm{cm}$	$360°/\,\mathrm{cm}$

Table 1: Structural parameters q and fabrication tolerances Δq for a cross strip isolator experiment as sketched in Figure 1. Δq corresponds to limits for isolation and loss of 20 dB and 1 dB. See the text for a concise interpretation of the limits for the parameter deviations.

By 'tolerances' we denote the parameter deviations, which are allowed such that the experiment can be carried out successfully, i.e. where one can exceed certain limits of isolation and loss by shifting the input focus. Successively for one of the paramters $q \in t, h, \lambda, n_\mathrm{s}, n_\mathrm{b}, n_\mathrm{t}, n_\mathrm{c}, \Theta_\mathrm{b}^\mathrm{F}, \Theta_\mathrm{t}^\mathrm{F}$ the tolerances Δq are estimated such that $\widetilde{\mathrm{IS}}_{q+\delta q}(L_0) \geq 20\,\mathrm{dB}$ and $\widetilde{\mathrm{LO}}_{q+\delta q}(L_0) \leq 1\,\mathrm{dB}$ for deviations δq with $-\Delta q \leq \delta q \leq \Delta q$. Directly evaluating the envelopes (4) for $L = L_0$ yields the tolerance limits for L_0. Table 1 summarizes a set of reasonable isolator parameters and the corresponding tolerances. Note that 'loss' refers to the field mismatch at the waveguide junctions only.

For a real device, material absorption, incoupling losses, etc. would have to be added. In the framework of the present overlap model, for tuned parameters the experiment should achieve an ideal isolation and an insertion loss of only $\mathrm{LO}_\mathrm{min} = 0.09\,\mathrm{dB}$. The nonreciprocal effect results in slightly different coupling lengths of $L_\mathrm{c}^\mathrm{f} = 4.5008\,\mu$m and $L_\mathrm{c}^\mathrm{b} = 4.4973\,\mu$m for opposite directions of propagation.

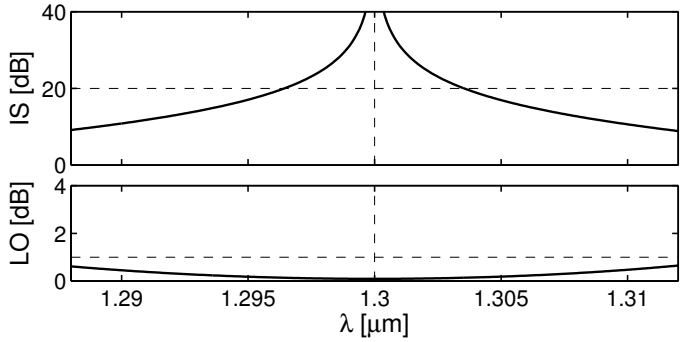

Figure 5: Isolation IS and loss LO versus the vacuum wavelength, for a tuned nonreciprocal cross strip interferometer according to Table 1.

The proposed tuning mechanism allows to compensate deviations in the film thicknesses, etching depth, the strip width, and in the material parameters that occur during the fabrication process. In principle it allows also to correct a drift of the (constant) wavelength that is applied in the experiment; the tolerance value $\Delta\lambda$ in Table 1 refers to that setting. However, for an application in a telecommunication setup, the *fixed* device has to work for a certain frequency range; any tuning technique can adjust optimum performance for a specific central wavelength only. Figure 5 shows that proper operation can be expected in a wavelength interval of about 8 nm around the design wavelength of $1.3\,\mu$m, if one demands an isolation level above 20 dB. This wavelength range will be relevant for the final application.

5 Radiation and reflection

Regarding the abrupt waveguide junctions, one might question the results of the previous model, since it neglects the reflected parts of the electromagnetic field completely, and includes the radiated fields only indirectly in terms of the overlap calculations. A rough estimation of these effects runs as follows.

For the interesting case of a tuned isolator operation, in the forward direction the intensity is concentrated in the lower film region at both junctions. The amounts of reflection and radiation should be low; they contribute to the inherent losses of the system. For backward light propagation, this applies to the input junction as well. At the second junction, the power is concentrated in the upper film region. Less than 15 % ($(n_\mathrm{t} - n_\mathrm{c})^2/(n_\mathrm{t} + n_\mathrm{c})^2$) of this power may be reflected, most of it into the radiation field, only a small fraction into the guided modes. The remaining part passes the junction, but it does not excite the guided output mode due to the almost vanishing overlap. If the following planar segment is of sufficient length, this power should leave the device. The

small guided part of the reflected power propagates (in the direction denoted as forward) towards the opposite junction, where again a fraction far below 15 % is reflected. Propagating backwards again, this part of less than 2 % of the input power may indeed reach the backward output. Fortunately this estimate of only 17 dB for the upper isolation limit turns out to be too pessimistic.

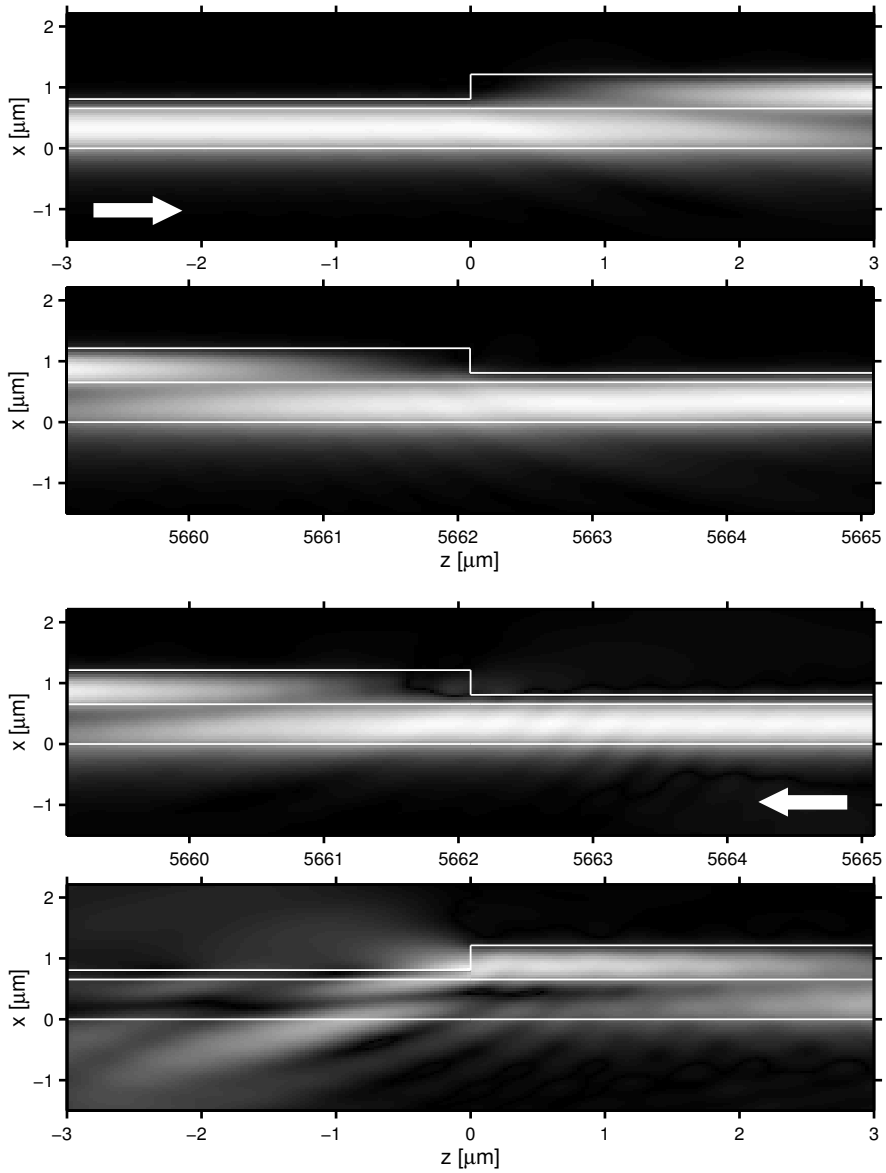

Figure 6: Simulation of the forward (top) and backward (bottom) light propagation through a cross strip as prescribed by Table 1, with a length of $L = 5.662$ mm. The gray scale levels correspond to the squareroot of the z-component of the local Poynting vector. In forward direction, almost the entire power passes the device, while the second junction scatters backward propagating waves into the surrounding.

We have checked the former considerations by applying the rigorous mode expansion technique as formulated in detail in Ref. [13]. Figure 6 illustrates the intensity distributions around the waveguide discontinuities for the two directions of light propagation. The simulations take full account of the reflected and radiated parts of the electromagnetic field. For the tuned setup with parameters as given in Table 1, we obtained a relative forward power transmission of 98 % and a relative reflected power of 0.03 %. In the blocking direction, a relative power of 0.27 % passes the device and a power fraction of 0.03 % is reflected. This amounts to an isolation ratio of 26 dB; the device suffers from forward losses of 0.1 dB. In particular, the results confirm that no further measures are required to alter the reflecting properties of the waveguide junctions.

6 Conclusions

A wide strip etched into a bimodal in plane double layer magnetooptic film may be viewed as a simple kind of nonreciprocal interferometer. By shifting the slightly trapezoidal strip in the lateral direction the device can be conveniently adjusted for optimum performance, if it is applied as an optical isolator. With the tuning

freedom allowed, we have estimated uncritical fabrication tolerances for the experimental setup. Note that the same relaxed limits apply, if the spatial shift is replaced by another tuning possibility, e.g. thermal treatment or subsequent etching.

A rigorous simulation predicts an isolation ratio of 26 dB and an insertion loss of 0.1 dB for a device operating at a wavelength of 1.3 μm. The low insertion loss and the small levels of reflections in either direction indicate that a sequencing of nonreciprocal cross strips, aiming at a higher isolation ratio or a wider frequency range, may be promising.

While the present design is basically a planar configuration, an extension to channel waveguides will be a subject of future research. Defining laterally weakly confining waveguides along the light path, e.g. by suitable annealing or by etching shallow ribs, seems to be unlikely to disturb the nonreciprocal properties of the interferometer. For first experiments with channel waveguides, selecting the optimum one of a couple of channels across a trapezoidal strip should enable tuning as in the planar case.

Acknowledgment

Financial support by Deutsche Forschungsgemeinschaft (Sonderforschungsbereich 225) is gratefully acknowledged.

References

[1] J. Warner. Nonreciprocal magnetooptic waveguides. *IEEE Transactions on Microwave Theory and Techniques*, MTT-23:70–78, 1975.

[2] R. Wolfe, R. A. Lieberman, V. J. Fratello, R. E. Scotti, and N. Kopylov. Etch-tuned ridged waveguide magneto-optic isolator. *Applied Physics Letters*, 56(5):426–428, 1990.

[3] M. Lohmeyer, N. Bahlmann, O. Zhuromskyy, H. Dötsch, and P. Hertel. Phase-matched rectangular magnetooptic waveguides for applications in integrated optics isolators: numerical assessment. *Optics Communications*, 158:189–200, 1998.

[4] F. Auracher and H. H. Witte. A new design for an integrated optical isolator. *Optics Communications*, 13(4):435–438, 1975.

[5] N. Bahlmann, M. Lohmeyer, O. Zhuromskyy, H. Dötsch, and P. Hertel. Nonreciprocal coupled waveguides for integrated optical isolators and circulators for TM-modes. *Optics Communications*, 161(4-6):330–337, 1999.

[6] J. Fujita, M. Levy, R. M. Osgood, L. Wilkens, and H. Dötsch. Waveguide optical isolator based on Mach-Zehnder interferometer. *Applied Physics Letters*, 76(16):2158–2160, 2000.

[7] A. F. Popkov, M. Fehndrich, M. Lohmeyer, and H. Dötsch. Nonreciprocal TE-mode phase shift by domain walls in magnetooptic rib waveguides. *Applied Physics Letters*, 72(20):2508–2510, 1998.

[8] N. Bahlmann, M. Lohmeyer, H. Dötsch, and P. Hertel. Finite-element analysis of nonreciprocal phase shift for TE modes in magnetooptic rib waveguides with a compensation wall. *IEEE Journal of Quantum Electronics*, 35(2):250–253, 1999.

[9] M. Fehndrich, A. Josef, L. Wilkens, J. Kleine-Börger, N. Bahlmann, M. Lohmeyer, P. Hertel, and H. Dötsch. Experimental investigation of the nonreciprocal phase shift of a TE-mode in a magneto-optic rib waveguide. *Applied Physics Letters*, 74(20):2918–2920, 1999.

[10] O. Zhuromskyy, M. Lohmeyer, N. Bahlmann, H. Dötsch, and P. Hertel. Analysis of polarization independent Mach-Zehnder type integrated optical isolator. *Journal of Lightwave Technology*, 17(7):1200–1205, 1999.

[11] O. Zhuromskyy, H. Dötsch, M. Lohmeyer, L. Wilkens, and P. Hertel. Magneto-optical waveguides with polarization independent nonreciprocal phase shift. *Journal of Lightwave Technology*, 2000. Submitted.

[12] N. Bahlmann, M. Lohmeyer, M. Wallenhorst, H. Dötsch, and P. Hertel. An improved design of an integrated optical isolator based on nonreciprocal Mach-Zehnder interferometry. *Optical and Quantum Electronics*, 30:323–334, 1998.

[13] M. Lohmeyer and R. Stoffer. Integrated optical cross strip polarizer concept. *Optical and Quantum Electronics*, 2000. Accepted for publication.

[14] S. Yamamoto and T. Makimoto. Circuit theory for a class of anisotropic and gyrotropic thin-film optical waveguides and design of non-reciprocal devices for integrated optics. *Journal of Applied Physics*, 45:882, 1974.

[15] M. Wallenhorst, M. Niemöller, H. Dötsch, P. Hertel, R. Gerhardt, and B. Gather. Enhancement of the nonreciprocal magneto-optic effect of TM modes using iron garnet double layers with opposite Faraday rotation. *Journal of Applied Physics*, 77(7):2902–2905, 1995.

[16] H. Dötsch, P. Hertel, B. Lührmann, S. Sure, H. P. Winkler, and M. Ye. Applications of magnetic garnet films in integrated optics. *IEEE Transactions on Magnetics*, 28(5):2979–2984, 1992.

[17] M. Shamonin and P. Hertel. Analysis of non-reciprocal mode propagation in magneto-optic rib-waveguide structures with the spectral-index method. *Applied Optics*, 33(27):6415–6421, 1994.